SOFT ROBOTS

Robotic metamorphosis by origami exoskeletons

Shuhei Miyashita,[1,2]* Steven Guitron,[1] Shuguang Li,[1] Daniela Rus[1]*

Changing the inherent physical capabilities of robots by metamorphosis has been a long-standing goal of engineers. However, this task is challenging because of physical constraints in the robot body, each component of which has a defined functionality. To date, self-reconfiguring robots have limitations in their on-site extensibility because of the large scale of today's unit modules and the complex administration of their coordination, which relies heavily on on-board electronic components. We present an approach to extending and changing the capabilities of a robot by enabling metamorphosis using self-folding origami "exoskeletons." We show how a cubical magnet "robot" can be remotely moved using a controllable magnetic field and hierarchically develop different morphologies by interfacing with different origami exoskeletons. Activated by heat, each exoskeleton is self-folded from a rectangular sheet, extending the capabilities of the initial robot, such as enabling the manipulation of objects or locomotion on the ground, water, or air. Activated by water, the exoskeletons can be removed and are interchangeable. Thus, the system represents an end-to-end (re)cycle. We also present several robot and exoskeleton designs, devices, and experiments with robot metamorphosis using exoskeletons.

INTRODUCTION

Some life forms have inherent metamorphic capabilities and acquire different functionalities in their developmental stages. Butterflies and beetles morph from larva and acquire the ability to fly (*1*). Hermit crabs switch their housings on demand, obtain materials from the environment, and change parts of their body. In comparison, most current hard-bodied machines, such as today's industrial robots, have a fixed architecture and cannot develop on-the-fly new functionalities. Inspired by nature, roboticists have designed self-reconfiguring robots, which are cellular machines consisting of a set of identical unit modules that can change their body geometry independently to match the structure to the task (*2*–*12*) or adapt their hardware and software in real time (*13*–*15*). Robots that aim for a flexible architecture have also been designed to deliver multiple locomotion modalities through several means: (i) by equipping them with redundant components (*16*–*19*), (ii) by constructing structures or tools on site (*20*, *21*), (iii) by designing modular systems capable of self-reconfiguration (*22*–*24*), or (iv) by creating origami-inspired bodies with programmable configurations (*6*–*8*, *10*, *25*–*30*). Each of these approaches can achieve a wide range of malleable capabilities (*31*, *32*), but in practice, extending the inherent physical capabilities of robots is challenging because of the electromechanical limitations of the robot body and the lack of (re)productivity of physical elements. Using metamorphosis in nature as an inspiration, we introduce an alternative approach to extending the capabilities of a robot by enabling it to cyclically acquire multiple self-folding origami sheets called "exoskeletons." Like an egg, the system commences with a cubic magnet "robot" called Primer. This robot hierarchically develops its morphology by combining with different exoskeletons; for example, it moves faster, becomes bigger, or uses different locomotion processes on the ground, in the water, and in the air. An example of metamorphosis is shown in Fig. 1, where Primer develops morphology through the processes of equipping exoskeletons; as a result, it obtains the ability to walk and roll. Removing an exoskeleton, analogous to insect molting, can be done by directing the robot into water, which dissolves the holding arms of the exoskeleton.

Our previous work contributes knowledge on static origami structures achievable from a single sheet (*6*) and mobile origami systems, where the body has a fixed origami structure and a fixed function (*8*, *29*). Here, we contribute to the concepts of robot metamorphosis using exoskeletons, specific designs and devices capable of metamorphosis, and end-to-end experiments and demonstrate how one shared origami structure acts as an "engine" capable of adding and removing different exoskeletons to achieve different body shapes and functions. The convergence of materials and machines enables this approach to be robotic metamorphosis by combining a compact design for function, efficient reconfiguration, and a large space for achievable, fine-resolution body shapes. The proposed approach demonstrates the advantages of origami-inspired manufacturing, namely, versatility, (re-)usability, and accessibility of components (*33*), which provide simplicity and structural redundancy to the mechanism.

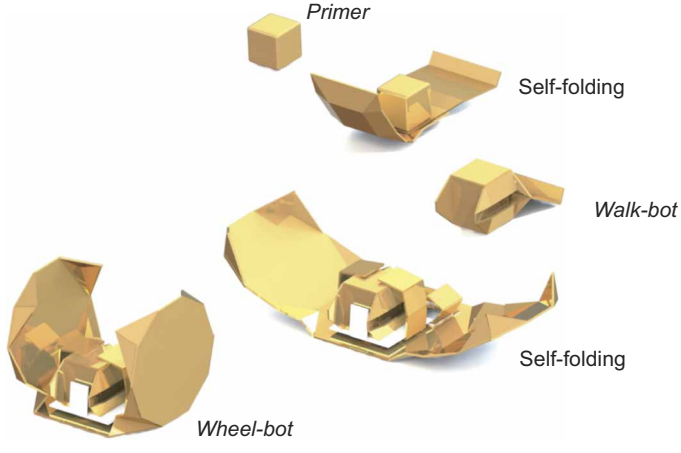

Fig. 1. Example of robotic metamorphosis by origami exoskeletons. Primer metamorphoses into Walk-bot and then to Wheel-bot, hierarchically equipping and obtaining different locomotion capabilities.

[1]Computer Science and Artificial Intelligence Laboratory, Massachusetts Institute of Technology, 32 Vassar Street, Cambridge, MA 02139, USA. [2]Department of Electronic Engineering, University of York, Heslington, York YO10 5DD, UK.
*Corresponding author. Email: shuhei.miyashita@york.ac.uk (S.M.); rus@csail.mit.edu (D.R.)

RESULTS

We demonstrate robotic metamorphosis with a suite of acquisitions and removals of robot exoskeletons. Each exoskeleton is designed to generate a different robot morphology that supports different capabilities. The system consists of Primer, an environment with a controllable magnetic field that enables the movement of the robot, two heating pads (Peltier element) for assembling the exoskeletons, a water reservoir for removing the exoskeleton, and a ramp for assisting gliding. The representative sequences for this system are shown in Fig. 2, with a scaling up of the body size (Fig. 2, A to F) and gliding performance (Fig. 2, G and H). The ability to walk is useful when the maintenance of posture is necessary (for example, when carrying a load, pushing an object, or acting as a patch in vivo) (*32*), where a small step size is needed. Acquiring large body sizes allows various abilities, such as faster walking, large-object transport, or stability against turbulence. A typical exoskeleton acquisition takes about 3 min to complete, and a typical molting process completes in less than a minute with the assistance of body vibration.

The transformations of the robot are shown as a state diagram in Fig. 3; origami self-folding robots can cyclically acquire modalities for walking (Walk-bot), scaling by a large homothetic exoskeleton (Scaled Walk-bot), rolling by cylindrical morphology (Wheel-bot), sailing on water by boat morphology (Boat-bot), and gliding in the air by wing morphology (Glider-bot). The scaling exoskeleton Scaled Walk-bot allows Walk-bot to move faster and shovel objects. The wheel exoskeleton gives Walk-bot two flat circular structures on both sides of the body, which act as wheels. It can roll on a plane 2.3 times faster than Walk-bot. The boat exoskeleton provides Walk-bot floating capability on water with enhanced buoyancy for a load carriage 1.86 times its own weight. Boat-bot features high side walls and a swept shape to maximize volumetric capacity underwater while minimizing drag. The glider exoskeleton endows Walk-bot with the capability to reach a distant place by gliding. As a dandelion distributes seeds blown by the wind or maple trees release propeller-shaped seeds that flutter down to reach a distance, the ability to glide would be useful when deploying robots or switching environments. Our experiments successfully demonstrate each end-to-end cycle that starts with Primer, extends Primer with one of the four exoskeletons, performs the capabilities enabled by the exoskeleton, and removes the exoskeleton.

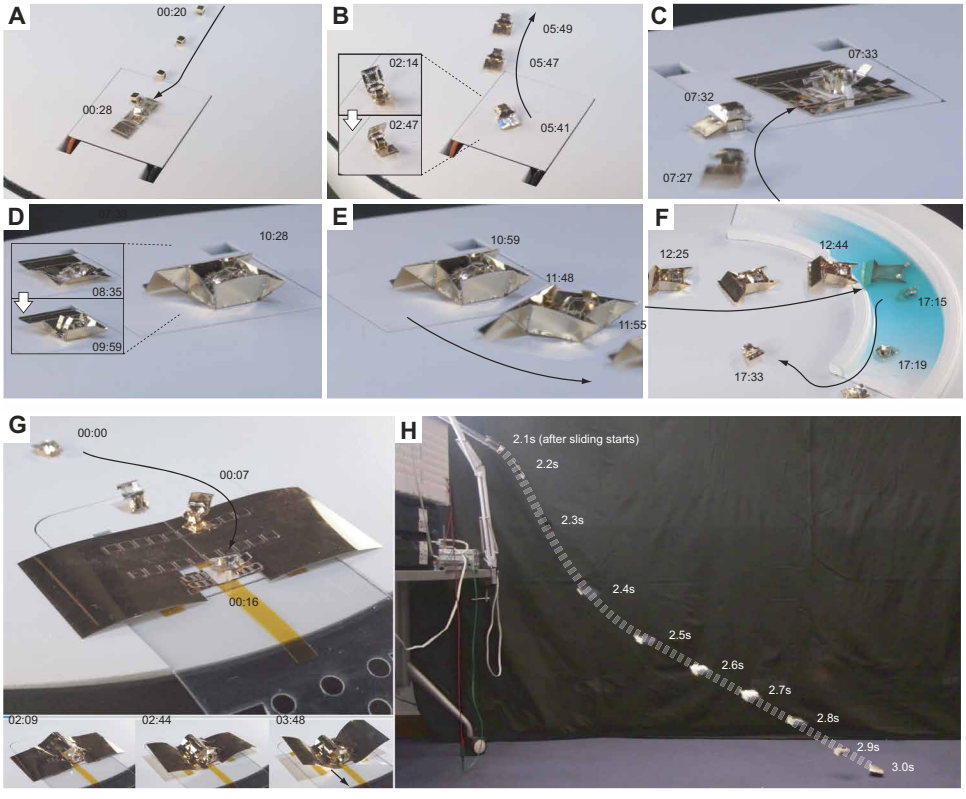

Fig. 2. Entire demonstrations of Scaled Walk-bot and Glider-bot. (**A**) Primer rolls remotely guided by a rotating magnetic field and can coalesce with Walk-bot self-folding sheet, the exoskeleton that encases and holds it. (**B**) Primer, which now features a minimal form for walking, supported by a tail for pitch stabilization, is forthwith capable of locomotion because of the eccentric body mass distribution (termed Walk-bot, the self-folding process in the small windows). (**C** and **D**) Walk-bot can further walk to another exoskeleton. The second exoskeleton can be equipped in the same way; it is held by self-folding arms that contain dissolving parts. After Walk-bot aligns on top of the latch module, the pit, four arms self-fold and hold Walk-bot such that Primer can transmit magnetic torque through the contact surface of the exoskeletons. At this point, the system morphs into a 2nd-shape (**E**), which has a larger but analogical morphology to Walk-bot (termed Scaled Walk-bot). (**F**) For "taking off" the second exoskeleton, Scaled Walk-bot enters a water reservoir where the four holding arms dissolve, and the released Walk-bot from the second exoskeleton can climb out of the reservoir and leave the exoskeleton discarded in the water. (**G** and **H**) Transformation of Walk-bot to Glider-bot and the gliding performance. Walk-bot acquires a wing and, assisted by a ramp, can reach 26 times its body length (129 cm) from the stage by gliding through the air from a height of 112 cm. See movies S1 to S4 for the entire experiments.

The comparison of the locomotion speeds of Walk-bot and Scaled Walk-bot at different magnetic field frequencies is shown in Fig. 4. With the periodic application of a magnetic field at angles of 27°, 63°, 90°, and −63° in the dorsal plane, both robots move on the stage in the direction of the magnetic field. Their walking speed reaches a maximum of 3.07 cm/s when a magnetic flux density 0.35 mT is applied at 9 Hz (0.34 cm per step). We applied a magnetic field five times stronger on Scaled Walk-bot than that on Walk-bot for pivoting, with the difference in the moment of inertia considered by reflecting the squares of distance between the pivot point and the center of the magnet. When a constant frequency oscillatory magnetic flux density of 1.75 mT is applied at 6 Hz, Scaled Walk-bot walks at a maximum speed of 4.66 cm/s (0.78 cm per step), which is 51.9% faster than the fastest speed of Walk-bot, supported by the 128% increase in step size. Walk-bot can walk faster with the Scaled Walk-bot exoskeleton. Scaled Walk-bot enables a larger step size. The larger step size allows us to use lower frequencies to achieve the same speed. The bigger step size is also useful for shoveling, moving a mass, and traveling over terrain with gaps. The other

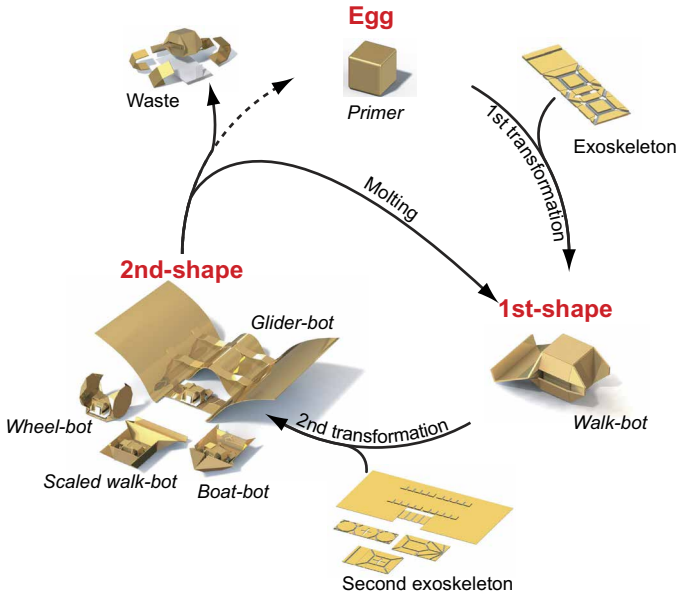

Fig. 3. Robotic metamorphic cycle. Starting as Primer at the top, the system morphs into the 1st-shape Walk-bot, as shown on the right. Walk-bot can subsequently transform into the 2nd-shape by integrating a self-folding exoskeleton. We demonstrate four capabilities—scaling up (Scaled Walk-bot), sailing (Boat-bot), rolling (Wheel-bot), and gliding (Glider-bot)—that can only be achieved by equipping exoskeletons, but other capabilities are also possible. The 2nd-shape can recover the morphologies of earlier stages by removing ("molting") the exoskeleton. The disassembly process of the second exoskeleton transforming to Walk-bot can be performed by dissolving the holding arms in water. The disassembly process of Walk-bot, which is beyond the scope of this study, can be performed by making the body of Walk-bot dissolvable to a specific solvent. We demonstrated this process with polyester-made origami robots that could dissolve relevant body parts after submersion in the solvent (*29*).

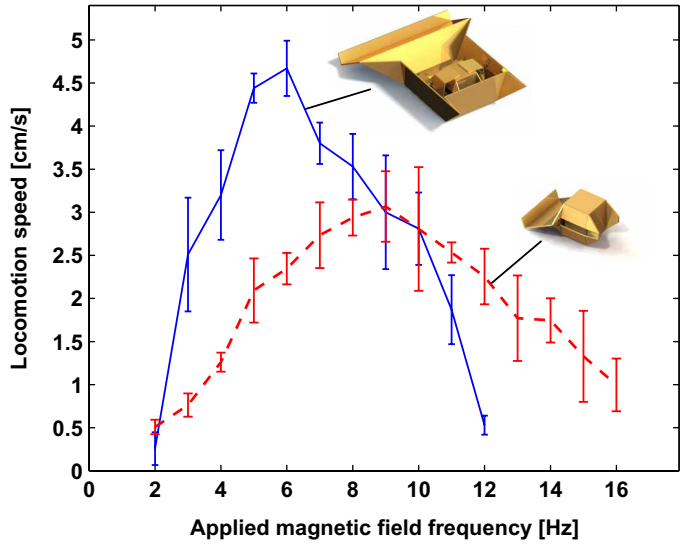

Fig. 4. Comparison of locomotion speeds between Walk-bot and Scaled Walk-bot. With the scaled morphology, an increase in walking speed of more than 50% was observed. Error bars indicate SD.

enhanced capabilities of the robot were quantitatively analyzed with respect to locomotion speed, floating capability, and gliding capability. For the details of each exoskeleton, see the Supplementary Materials.

DISCUSSION

Robots with fixed architectures will perform the task for which they are designed well but will perform poorly on different tasks in different environments. This study introduces the possibility of developing a robot that can extend and switch its capabilities by putting on exoskeletons and changing its body shape. We explored how the use of materials and a task-centered design can empower robots with a wide range of capabilities, with the complexity of the fixed robot body traded off with the design and control challenges of changing shape. The robot could acquire these capabilities to perform additional tasks, such as driving through water and burrowing or anchoring in sand. Exoskeletons could also form fixtures or simple tools, such as a drill, water scoop, shovel, cutter, or grabber. Likewise, they can potentially be used for biomimicry functions, such as tail cutting or camouflaging. The principle of on-site morphing with custom exoskeletons to rapidly create new types of robots has the potential to provide more flexibility to robotic operations at difficult-to-access sites in multiple fields, such as in space manufacturing, incision-free medical procedures (*32*), deep-sea construction, and disaster-site rescue operations. Although the devices demonstrated in this study are small in scale, robots with similar metamorphosis capabilities can be created using the same principles at a wide variety of scales.

Suppose a robot needs to execute task A, which requires (for example) traversing water, followed by task B, which requires shoveling an area. Instead of creating a robot whose body can execute tasks A and B simultaneously, we propose designing a simpler robot, Primer, that can act as the engine for a multitude of tasks. Each task has a corresponding exoskeleton designed to wrap around and connect to Primer. Primer can pick up the exoskeleton by using a self-folding process activated by heat and remove it by using a self-disassembly process activated by water. For our example tasks A and B, Primer acts as the engine that can travel to pick up the exoskeleton for task A (sailing), execute the sailing task, drive to discard the exoskeleton for sailing upon completion of this task, drive to pick up the exoskeleton for task B (shoveling), and continue. The key insight in this work is that through the use of novel materials that can be self-folded and self-disassembled, we simplified the design of robot systems while increasing the range of tasks that they can perform. The key technical contributions of our study include (i) developing the design of Primer and exoskeletons for scaling the robot to move with larger steps, shoveling, rolling, sailing, and gliding; (ii) creating the methods for acquiring and removing exoskeletons; and (iii) conducting end-to-end experiments for robot metamorphosis and task execution for each capability.

The capabilities of robots are defined by what their bodies can do and how their "brains" can control these bodies to execute tasks. The body, the brain, and the tasks that can be executed have a tight coupling. We believe that this work will open the door to the development of a new class of robots that are compact and can be specialized and customized to execute a wide range of tasks. This study demonstrates on-site, on-demand robotic morpho-functional acquisition and disposal achieved purely on a material basis, in which the same material unit can be used to flexibly add and remove a part of the structure and reshape its operative boundary.

MATERIALS AND METHODS

The platform and experimental condition

Figure 5 shows the newly designed platform, which provides an environment for testing the robot. It consists of a stage, two Peltier elements for robot self-assembly, a water reservoir for robot disassembly and sailing experiments, a ramp on which Glider-bot slides for gliding, a motor-assisted leaning pad (Servo motor HS-55, Hitec) positioned adjacent to the ramp to initiate the slide, four solenoid coils (diameter, 21 cm) inclined 45° from the horizontal plane (directed toward the center of the stage from beneath), and the supporting electronics for current control. The stage is 30 cm in diameter with an actuatable workspace of 25 cm. The water reservoir is an arc-shaped lane sloping down toward the middle part. A robot can enter and exit the reservoir from either side, or it can directly jump in from the middle part where no protection wall exists. The deepest part is 1.52 cm in depth, and the average slope angle is 10°. The ramp has a traveling length of 47 cm for Glider-bot, and it is set at an inclination angle of 33° from the horizontal plane. Glider-bot is released at a height of 112 cm from the ground. The currents for producing magnetic fields are controlled with a microcontroller (Arduino Esplora) and four motor drivers (SyRen25, Dimension Engineering) through serial communication.

The remote actuation of the robot is possible by transferring magnetic force and torque to Primer with the electromagnetic coils (*34*–*43*). The platform used in the experiments for this work provides a significantly wider range of controllable space; most of the other coil systems were developed to cover merely several centimeters of workspace. The attachment mechanisms of the exoskeletons require precise localization, which can be provided via magnetic sensing, vision, or an external tracking and localization system. Whereas autonomous localization using magnetic sensing was demonstrated in our platform in (*44*), in this work, we focus on the metamorphosis of robots and reduce experimental complexity by relying on a human operator to remotely control the alignment between the robot and its exoskeletons, and the direction of the robot's movement. The patterns of the applied magnetic fields are adjusted to each locomotion modality to reflect the dynamics and body mass (see the Supplementary Materials for details).

Using the control mechanism, we conducted five end-to-end experiments for each design. We started with Primer, created Walk-bot (1st-shape), created 2nd-shape extended from Walk-bot, demonstrated the new capabilities, and transformed the robot from the 2nd-shape to the 1st-shape. We also conducted multiple experiments for the respective transitions and consistently achieved success. During these experiments, the biggest challenge was the accurate alignment control of Walk-bot to the exoskeleton sheet, which is required to transition from one shape to another.

Self-folding

The self-folding of exoskeletons is achieved using the tensile stress of a prestretched thermo-shrinking polymer film (polyvinyl chloride, deformation occurs at 65°C, 0.03 mm thickness, Shrink Bag), laminated on both sides with two rigid sheets (Mylar sheets, 0.05 mm thickness, Mylar) by using silicone adhesive (High-Temperature Glue-on-a-Roll, McMaster-Carr). By differentiating the crease widths on the front and back sides of the self-folding sheet pattern, the folding direction can be controlled (*45*). When the sheet is exposed to heat at the glass transition temperature or marginally higher, a difference in shear stress is induced in the contractive layer between the

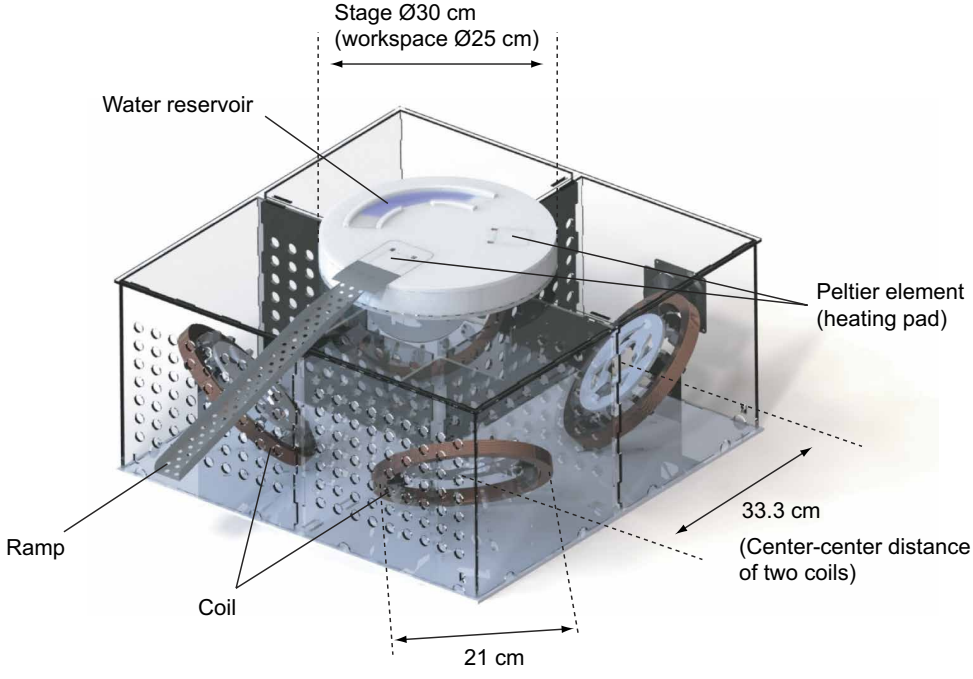

Fig. 5. The platform, which consists of four solenoid coils, two Peltier elements, a water reservoir, and a ramp.

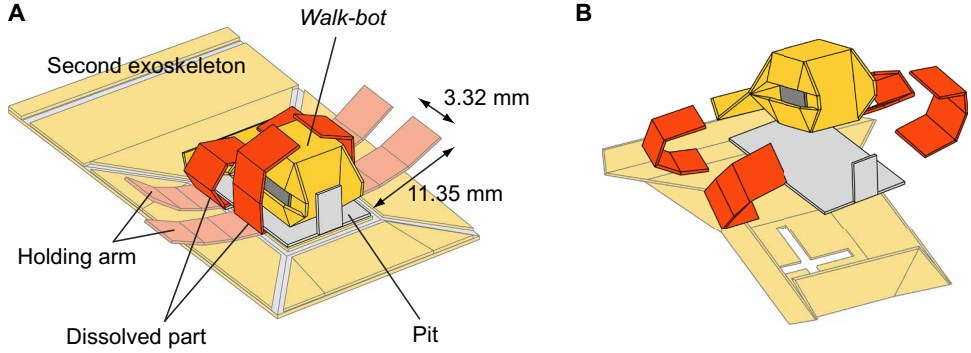

Fig. 6. Docking and molting mechanism. (**A**) Four arms, whose roots are made of water-dissolvable material, tightly hold Walk-bot. (**B**) Upon immersion in water, the roots dissolve and release Walk-bot.

two opposite faces, where the side with a wider gap contracts more and, in turn, creates a fold (*45*). All the creases are designed to fold simultaneously, but they experience speed differences, depending on the loads placed on the creases and the distance from the Peltier element. The fabrication of self-folding sheets is completed using a computer-aided cutting process with either a laser cutter or vinyl cutter and manual lamination processes. The Peltier elements (Therma TEC 926-1279-ND, Laird Technologies) used are 43.9 cm × 39.9 cm in size and can differentiate up to 63°C between both faces. The temperature rise is triggered manually with a constant current (2.2 A) to the respective elements in an open-loop manner.

Docking and "molting" mechanism

A holding arm/latch assembly equipped in the exoskeleton sheet enables Walk-bot to interface with the exoskeleton. The assembly consists of four latches: two front latches are longer to wrap around Primer of Walk-bot, whereas two back latches hold the tail of Walk-bot tightly to allow the torque to be transmitted through the structure (Fig. 6). The two front arms have wide, connected segments so that, during the self-folding process, they can stay rigid enough to completely encase the magnet. The two back arms have thin, disconnected segments so that they can fold over the low tail. The roots of the arms were made of water-soluble paper, ASWT-1 (Aquasol). When exposed to water, the water-soluble tape dissolves; it separates the arms from the exoskeleton and enables Walk-bot to be released. In our investigation, dissolving a latch from the body by physically vibrating the exoskeleton at 2 Hz took 18 s (five samples), on average. In the experiments, 5 min was allotted to allow all latch connections to completely dissolve.

SUPPLEMENTARY MATERIALS

robotics.sciencemag.org/cgi/content/full/2/10/eaao4369/DC1
Materials and Methods
Fig. S1. The platform.
Fig. S2. Walk-bot design.
Fig. S3. Scaled Walk-bot design.
Fig. S4. Wheel-bot design.
Fig. S5. The rolling speed of Wheel-bot over frequency of magnetic field applied (five samples).
Fig. S6. Demonstration of Wheel-bot.
Fig. S7. Boat-bot design.
Fig. S8. Demonstration with boat exoskeleton.
Fig. S9. Glider-bot design.
Table S1. Success and failure events with Scaled Walk-bot.
Table S2. Success and failure events with Wheel-bot.
Table S3. Success and failure events with Boat-bot.
Table S4. Success and failure events with Glider-bot.
Movie S1. Scaled Walk-bot as shown in Fig. 2.
Movie S2. Wheel-bot as shown in fig. S6.
Movie S3. Boat-bot as shown in fig. S8.
Movie S4. Glider-bot as shown in Fig. 2.
Reference (*46*)

REFERENCES AND NOTES

1. N. A. Campbell, J. B. Reece, L. Urry, M. L. Cain, S. A. Wasserman, P. V. Minorsky, R. B. Jackson, *Biology: A Global Approach* (Pearson, 2014).
2. K. Kotay, D. Rus, M. Vona, C. McGray, The self-reconfiguring robotic molecule, in *Proceedings of the IEEE/RSJ International Conference on Intelligent Robots and Systems (IROS)* (IEEE, 1998), pp. 424–431.
3. S. Murata, H. Kurokawa, Self-reconfigurable robots. *IEEE Robot. Autom. Mag.* **14**, 71–78 (2007).
4. K. Gilpin, A. Knaian, D. Rus, Robot pebbles: One centimeter module for programmable matter through self-disassembly, in *Proceedings of the IEEE International Conference on Robotics and Automation (ICRA)* (IEEE, 2010), pp. 2485–2492.
5. M. Yim, W.-m. Shen, B. Salemi, D. Rus, M. Moll, H. Lipson, E. Klavins, G. S. Chrikjian, Modular self-reconfigurable robot systems. *IEEE Robot. Autom. Mag.* **14**, 43–52 (2007).
6. E. Hawkes, B. An, N. M. Benbernou, H. Tanaka, S. Kim, E. D. Demaine, D. Rus, R. J. Wood, Programmable matter by folding. *Proc. Natl. Acad. Sci. U.S.A.* **107**, 12441–12445 (2010).
7. C. D. Onal, M. T. Tolley, R. J. Wood, D. Rus, Origami-inspired printed robots. *IEEE/ASME Trans. Mech.* **20**, 2214–2221 (2014).
8. S. Felton, M. T. Tolley, E. Demaine, D. Rus, R. J. Wood, A method for building self-folding machines. *Science* **345**, 644–646 (2014).
9. A. Firouzeh, J. Paik, Robogami: A fully integrated low-profile robotic origami. *J. Mech. Robot.* **7**, 021009 (2015).
10. K. C. Cheung, E. D. Demaine, J. R. Bachrach, S. Griffith, Programmable assembly with universally foldable strings (moteins). *IEEE Trans. Robot.* **27**, 718–729 (2011).
11. A. Cully, J. Clune, D. Tarapore, J.-B. Mouret, Robots that can adapt like animals. *Nature* **521**, 503–507 (2015).
12. M. Boyvat, J.-S. Koh, R. J. Wood, Addressable wireless actuation for multijoint folding robots and devices. *Sci. Robot.* **2**, eaan1544 (2017).
13. H. Lipson, J. B. Pollack, Automatic design and manufacture of artificial lifeforms. *Nature* **406**, 974–978 (2000).
14. V. Zykov, E. Mutilinaios, B. Adams, H. Lipson, Self-reproducing machines. *Nature* **435**, 163–164 (2005).
15. J. Bongard, Morphological change in machines accelerates the evolution of robust behavior. *Proc. Natl. Acad. Sci. U.S.A.* **108**, 1234–1239 (2011).
16. J. D. Dickson, J. E. Clark, Design of a multimodal climbing and gliding robotic platform. *IEEE/ASME Trans. Mech.* **18**, 494–505 (2013).
17. M. A. Woodward, M. Sitti, MultiMo-Bat: A biologically inspired integrated jumping-gliding robot. *Int. J. Robot. Res.* **33**, 1511–1529 (2014).
18. A. Vidyasagar, J.-C. Zufferey, D. Floreano, M. Kovač, Performance analysis of jump-gliding locomotion for miniature robotics. *Bioinspir. Biomim.* **10**, 025006 (2015).
19. K. Jayaram, R. J. Full, Cockroaches traverse crevices, crawl rapidly in confined space, and inspire a soft, legged robot. *Proc. Natl. Acad. Sci. U.S.A.* **113**, E950–E957 (2016).
20. S. Revzen, M. Bhoite, A. Macasieb, M. Yim, Structure synthesis on-the-fly in a modular robot, in *Proceedings of the IEEE/RSJ International Conference on Intelligent Robots and Systems (IROS)* (IEEE, 2011), pp. 4797–4802.
21. L. Wang, L. Brodbeck, F. Iida, Mechanics and energetics in tool manufacture and use: A synthetic approach. *J. R. Soc. Interface* **11**, 20140827 (2014).
22. J. Hiller, H. Lipson, Automatic design and manufacture of soft robots. *IEEE Trans. Robot.* **28**, 457–466 (2012).
23. E. Klavins, Programmable self-assembly. *IEEE Control Syst. Mag.* **27**, 43–56 (2007).
24. J. W. Romanishin, K. Gilpin, D. Rus, M-blocks: Momentum-driven, magnetic modular robots, in *Proceedings of the IEEE/RSJ International Conference on Intelligent Robots and Systems (IROS)* (IEEE, 2013), pp. 4288–4295.
25. I. Shimoyama, H. Miura, K. Suzuki, Y. Ezura, Insect-like microrobots with external skeletons. *IEEE Control Syst.* **13**, 37–41 (1993).
26. A. M. Hoover, E. Steltz, R. S. Fearing, RoACH: An autonomous 2.4g crawling hexapod robot, in *Proceedings of the IEEE/RSJ International Conference on Intelligent Robots and Systems (IROS)* (IEEE, 2008), pp. 26–33.
27. J. P. Whitney, P. S. Sreetharan, K. Y. Ma, R. J. Wood, Pop-up book MEMS. *J. Micromech. Microeng.* **21**, 115021 (2011).
28. M. Noh, S.-W. Kim, S. An, J.-S. Koh, K.-J. Cho, Flea-inspired catapult mechanism for miniature jumping robots, *IEEE Trans. Robot.* **28**, 1007–1018 (2012).
29. S. Miyashita, S. Guitron, M. Ludersdorfer, C. R. Sung, D. Rus, An untethered miniature origami robot that self-folds, walks, swims, and degrades, in *Proceedings of the IEEE International Conference on Robotics and Automation (ICRA)* (IEEE, 2015), pp. 1490–1496.
30. J. Morgan, S. P. Magleby, L. L. Howell, An approach to designing origami-adapted aerospace mechanisms, *J. Mech. Des.* **138**, 052301 (2016).
31. K. Kuribayashi, K. Tsuchiya, Z. You, D. Tomus, M. Umemoto, T. Ito, M. Sasaki, Self-deployable *origami* stent grafts as a biomedical application of Ni-rich TiNi shape memory alloy foil. *Mater. Sci. Eng. A* **419**, 131–137 (2006).
32. S. Miyashita, S. Guitron, K. Yoshida, S. Li, D. D. Damian, D. Rus, Ingestible, controllable, and degradable origami robot for patching stomach wounds, in *Proceedings of the IEEE International Conference on Robotics and Automation (ICRA)* (IEEE, 2016), pp. 909–916.
33. R. J. Lang, *Origami Design Secrets* (CRC Press, 2012).
34. T. Honda, K. I. Arai, K. Ishiyama, Micro swimming mechanisms propelled by external magnetic fields. *IEEE Trans. Magn.* **32**, 5085–5087 (1996).
35. K. Ishiyama, M. Sendoh, K. I. Arai, Magnetic micromachines for medical applications. *J. Magn. Magn. Mater.* **242–245**, 41–46 (2002).
36. S. Martel, J.-B. Mathieu, O. Felfoul, A. Chanu, E. Aboussouan, S. Tamaz, P. Pouponneau, Automatic navigation of an untethered device in the artery of a living animal using a conventional clinical magnetic resonance imaging system. *Appl. Phys. Lett.* **90**, 114105 (2007).

37. K. Vollmers, D. R. Frutiger, B. E. Kratochvil, B. J. Nelson, Wireless resonant magnetic microactuator for untethered mobile microrobots. *Appl. Phys. Lett.* **92**, 144103 (2008).
38. C. Pawashe, S. Floyd, M. Sitti, Modeling and experimental characterization of an untethered magnetic micro-robot. *Int. J. Robot. Res.* **28**, 1077–1094 (2009).
39. M. P. Kummer, J. J. Abbott, B. E. Kratochvil, R. Borer, A. Sengul, B. J. Nelson, OctoMag: An electromagnetic system for 5-DOF wireless micromanipulation, in *Proceedings of the IEEE International Conference on Robotics and Automation (ICRA)* (IEEE, 2010), pp. 1006–1017.
40. S. Miyashita, E. Diller, M. Sitti, Two-dimensional magnetic micro-module reconfigurations based on inter-modular interactions. *Int. J. Robot. Res.* **32**, 591–613 (2013).
41. E. Diller, J. Giltinan, G. Z. Lum, Z. Ye, M. Sitti, Six-degree-of-freedom magnetic actuation for wireless microrobotics. *Int. J. Robot. Res.* **35**, 114–128 (2015).
42. B. E. Kratochvil, D. R. Frutiger, K. Vollmers, B. J. Nelson, Visual servoing and characterization of resonant magnetic actuators for decoupled locomotion of multiple untethered mobile microrobots, in *Proceedings of the IEEE International Conference on Robotics and Automation (ICRA)* (IEEE, 2009), pp. 1010–1015.
43. E. Diller, J. Giltinan, M. Sitti, Independent control of multiple magnetic microrobots in three dimensions. *Int. J. Robot. Res.* **32**, 614–631 (2013).
44. S. Guitron, A. Guha, S. Li, D. Rus, Autonomous locomotion of a miniature, untethered origami robot using hall effect sensor-based magnetic localization, in *Proceedings of the IEEE International Conference on Robotics and Automation (ICRA)* (IEEE, 2017), pp. 4807–4813.
45. S. Miyashita, C. D. Onal, D. Rus, Self-pop-up cylindrical structure by global heating, in *Proceedings of the IEEE/RSJ International Conference on Intelligent Robots and Systems (IROS)* (IEEE, 2013), pp. 4065–4071.
46. C. Sung, R. Lin, S. Miyashita, S. Yim, S. Kim, D. Rus, Self-folded soft robotic structures with controllable joints, in *Proceedings of the IEEE International Conference on Robotics and Automation (ICRA)* (IEEE, 2017), pp. 580–587.

Funding: This study was supported by NSF grants 1240383 and 1138967. **Author contributions:** S.M. and S.L. conceived the concept; S.M., S.L., and D.R. designed the research; S.M., S.G., and S.L. developed the system; S.G. and S.L. performed the experiments; S.G. analyzed the data; and S.M., S.G., and D.R. wrote the paper. D.R. provided funding. **Competing interests:** The authors declare that they have no competing interests. **Data and materials availability:** Contact S.M. for other materials.

Submitted 20 July 2017
Accepted 11 September 2017
Published 27 September 2017
10.1126/scirobotics.aao4369

Citation: S. Miyashita, S. Guitron, S. Li, D. Rus, Robotic metamorphosis by origami exoskeletons. *Sci. Robot.* **2**, eaao4369 (2017).

Science Robotics

Robotic metamorphosis by origami exoskeletons

Shuhei Miyashita, Steven Guitron, Shuguang Li, and Daniela Rus

Sci. Robot. **2** (10), eaao4369. DOI: 10.1126/scirobotics.aao4369

Science Robotics (ISSN 2470-9476) is published by the American Association for the Advancement of Science. 1200 New York Avenue NW, Washington, DC 20005. The title *Science Robotics* is a registered trademark of AAAS.